

Electrochemical-DNA Biosensor Development Based on a Modified Carbon Electrode with Gold Nanoparticles for Influenza A (H1N1) Detection: Effect of Spacer

Hyo-Eun Lee, Yun Ok Kang, Seong-Ho Choi*

Department of Chemistry, Hannam University, Daejeon 305-811, Republic of Korea

*E-mail: shchoi@hnu.kr

Received: 9 April 2014 / Accepted: 25 August 2014 / Published: 29 September 2014

An Electrochemical-DNA biosensor (E-DNA biosensor) was prepared successfully for electrochemical detection of a target DNA sequence, and the effective surface of the electrode was designed in order to achieve high sensitivity. First, electrode surfaces were modified chemically for immobilization of biomolecules by electrochemical reduction of 4-thiophenyl diazonium salt without any reducing agents. The thiol-modified electrode (TP-GCE) may be used to immobilize functionalized gold nanoparticles (Au NPs) and biomolecules. The characteristics of the modified electrode were obtained using cyclic voltammetry, contact angle, AFM, and XPS analysis. For confirmation of the effective influence of self-assembled layers (SAMs) with sensitivity of E-DNA biosensor, the spacer effect was determined by forming SAMs layer with 3-mercaptopropionic acid (MPA) and 11-mercaptopundecanoic acid (MUA) on the electrode. The E-DNA biosensor based on the MUA-modified electrode performed with higher sensitivity in hybridization between the probe DNA on the electrode and the target DNA than that based on the MPA-modified electrode because of the spacer effect that occurred owing to the long chemical chain of the MPA molecules. The new E-DNA biosensor is considered as the one of the most promising materials for highly sensitive clinical and other biotechnology applications.

Keywords: E-DNA biosensor, Electrochemical reaction, Hybridization, Influenza virus (type A), 11-mercaptopundecanoic acid (MUA)

1. INTRODUCTION

The DNA biosensor is considered a promising tool in pre-diagnosis, and in the prevention and control of infectious diseases by offering a promising alternative for faster, cheaper, and simpler nucleic acid assays in comparison with transitional methods, such as polymerase chain reaction (PCR), reverse transcription polymerase chain reaction (RT-PCR), or electrophoresis [1-3]. Over the past few

years, various types of highly sensitive and selective DNA sensors developed. The detection of a DNA sequence by this type of sensor has been described based on optical, gravimetric, acoustic, and electrochemical processes. The E-DNA biosensor is known in particular as a promising tool for various applications such as clinical diagnosis, reliable forensic analysis, environmental monitoring, and biological research because of its high sensitivity, compatibility with modern micro-fabrication technologies, low cost, portability, and label-free design [4-6].

Influenza A viruses, which appeared in Mexico by 2009 and then rapidly spread around the world, cause respiratory disease and are spreads by physical contact and through the air in public places. The enzyme-linked immunosorbent assay (ELISA) is common method for the detection of Influenza A [7-8]. Although this method can provide the desired sensitivity, specificity, and selectivity, in general it is highly disadvantageous because it requires the labelling of an antigen or antibody, long analysis times, and extensive sample handling. The formation of modified influenza A virus antigenicity could also lead to significant difficulties in detection [9]. Accordingly, there is a need to develop an assay method that has high sensitivity, selectivity, and rapidity at early diagnosis was required to protect from infection as soon as possible.

Recently, we grafted phenyl carboxylic acid onto different electrodes, such as indium tin oxide (ITO), gold (Au), and glassy carbon electrode (GCE). Subsequently, an electrochemical DNA sensor (E-DNA biosensor) based on the phenyl carboxylic acid-modified GCE was fabricated by the immobilization of probe DNA. The fabricated E-DNA biosensor can detect the influenza virus (type A). The current density of the E-DNA biosensor was evaluated by cyclic voltammetry when the probe DNA and target DNA were hybridized [4, 7]. It was found that 4-carboxyphenyl diazonium salts could be polymerized onto the surface of the GCE as a phenyl carboxylic acid back bone. The phenyl carboxylic acid polymer is one category of conjugate polymer; and this polymer can used as an electron transfer mediator on the electrode in order to increase electron transfer, while the carboxylic acid group of this polymer can be used to immobilize biomolecules, such as enzymes.

The combination of nanomaterials and biomolecules in a biorecognition process has attracted considerable attention. Nanoparticles of noble metals, especially gold nanoparticles (Au NPs), can play an important role in the construction of biosensors because of their large specific area, excellent biocompatibility, good conductivity capability, desirable catalytic properties, and small size [10-14]. For the fabrication of an E-DNA biosensor, Au NPs have been used and are one of most effective methods because this allows it let an electron movement between the electrode and biomolecules, while the and loading of Au NPs by thiol groups in an organic molecules was easy and simple technique.

Sulfur containing compounds, such as 3-mercaptopropionic acid (MPA) and 11-mercaptoundecanoic acid (MUA), are known to be suitable for the preparation a biosensor [2, 15-18] because their biofunctional molecules that contain both thiol and carboxylic acid groups are well known for serving as binding sites for covalent attachment to metal nanoparticles and also for reacting covalently with phosphate groups in DNA in order to achieve effective immobilization and increase lifetime stability. Numerous papers have addressed the formation of E-DNA sensor using either MPA or MUA, but the few studies have attempted to compare MPA and MUA to in the fabrication of a biosensor.

Here, a focus was centered on the investigation of spacer effect by SAMs layers composed of MPA and MUA to achieve effective immobilization of DNA. The electrochemical DNA biosensor based on an MPA or MUA-modified electrode was fabricated by an avidin-biotin reaction of biotinylated probe DNA. First, a thiol group was introduced on the glassy carbon electrode (GCE) by 4-thiophenyl diazonium, and then Au NPs were deposited by electrochemical modification of the thiol surface on the electrode. The self-assembled modification was formed using MPA or MUA to compare their efficiency as a biosensor, and a further coupling reaction using *N*-hydroxysuccinimide (NHS) and *N*-3-dimethyl aminopropyl)-*N'*-ethylcarbodiimide hydrochloride (EDC) was induced for hybridization with the target DNA, influenza A (H1N1).

2. EXPERIMENTAL

2.1. Materials

4-aminothiophenol, sodium nitrite (NaNO_2), $\text{HAuCl}_4 \cdot 4\text{H}_2\text{O}$, 3-Mercaptopropionic acid (MPA), 11-mercaptoundecanoic acid (MUA), *N*-hydroxysuccinimide (NHS), *N*-3-dimethyl aminopropyl)-*N'*-ethylcarbodiimide hydrochloride (EDC), avidin (from egg whites), and potassium hexacyanoferrate(II) trihydrate were purchased from Sigma-Aldrich Korea Ltd. Potassium ferrocyanide ($\text{K}_3\text{Fe}(\text{CN})_6$) and potassium chloride (KCl) were purchased from Duksan Pharma Ceutica Co., Ltd. Phosphate buffer solution (PBS) was prepared by mixing stock solutions of NaH_2PO_4 and Na_2HPO_4 , and then adjusting to pH7. All solutions for the experiments were prepared with water purified in a Milli-Q plus water purification system (Millipore Co. Ltd). The 24-base oligonucleotide biotinylated probe DNA, its complementary sequence DNA (target DNA, namely a 24-base fragment of an influenza virus gene sequence), and two-base mismatch DNA were purchased from the Bionics Company (Korea). Their base sequences are as described in Scheme 2. All oligonucleotides were dissolved in Tris-EDTA buffer solution (pH 8.0) and were kept frozen.

The probe sequence was 5'-biotin-ATG AGT CTT CTA ACC GAG GTC GAA-3' and the complementary target sequence was 5'-TTC GAC CTC GGT TAG AAG ACT CAT -3'. The sequence of two-base mismatch DNA employed was 5'-TTC GAC AGC GGT TAT AAG ACT CAT-3'.

2.2. Modification of glassy carbon electrode (GCE)

The immobilization of Au NPs on the surface of the GCE (Au-TP-electrode) is described in Scheme 1. 1 mM of 4-aminothiophenol and 1mM of sodium nitrite (NaNO_2) were dissolved in 10 ml of 0.5 M aqueous hydrochloride solution [19-20]. After the two reagents were mixed, the mixture solution was cooled to 0°C for 15 min. The electrode was modified by the following steps. The surface of the GCE was cleaned by polishing with 0.3 μm $\alpha\text{-Al}_2\text{O}_3$ powder. After each polishing, the electrode was washed with ultrapure water. Then the GCE by electrochemical reduction of diazonium through immersion on 1 mM of 4-thiophenyl diazonium for 10 min at -0.7 V. To immobilize the Au NPs, the 4-thiophenyl diazonium-modified GCE (TP-GCE) was subject to electrochemical reduction by

immersion for for 10 min at 0.4 V in 20 mL of 0.5 M H₂SO₄ solution containing 1.0 mM hydrogen tetrachloroaurate(III) hydrate (HAuCl₄·nH₂O, n=3.6). One Au NPs-modified electrode was immersed in ethanol solution containing 3-mercaptopropionic acid for two days at 0°C (MPA-Au-TP-GCE), while another Au NPs-modified electrode was immersed in ethanol solution containing 11-mercaptopundecanoic acid for two days at 0°C (MUA-Au-TP-GCE). Each of the MPA-modified electrode and MUA-modified electrode were immersed separately in PBS (pH 7.0) containing 30 mM EDC and 30 mM NHS for 2 h at room temperature according to an earlier reference [21]. After the electrode surface was washed with 0.1 M PBS, the electrodes were functionalized with avidin in a PBS containing 200 µg/mL avidin for 2 h at room temperature, and then rinsed with 0.1 M PBS.

2.3 Immobilization of biotinylated probe DNA onto the electrode and DNA hybridization on the probe DNA immobilized electrode

The avidin-modified electrode was immersed in 0.1 M PBS (pH 7.0) containing 10 pM biotinylated probe DNA for 1 h at room temperature in order to immobilize the biotinylated probe DNA. Then the biotinylated probe DNA immobilization on the avidin-modified electrode was washed with 0.1% SDS phosphate buffer for 5 min to remove the unbound DNA probes. For hybridization of the target DNA, the biotinylated probe DNA-modified electrode was immersed in 0.1 M PBS (pH 7.0) containing different concentrations of the target DNA for 45 min at 38°C. The electrode surface was washed with ultra-pure water and 0.1% SDS phosphate buffer for 5 min to remove the unbound oligonucleotides. The same protocol as above was applied to the probe DNA-immobilized electrodes for hybridization reactions of probe DNA with two-base mismatched DNA.

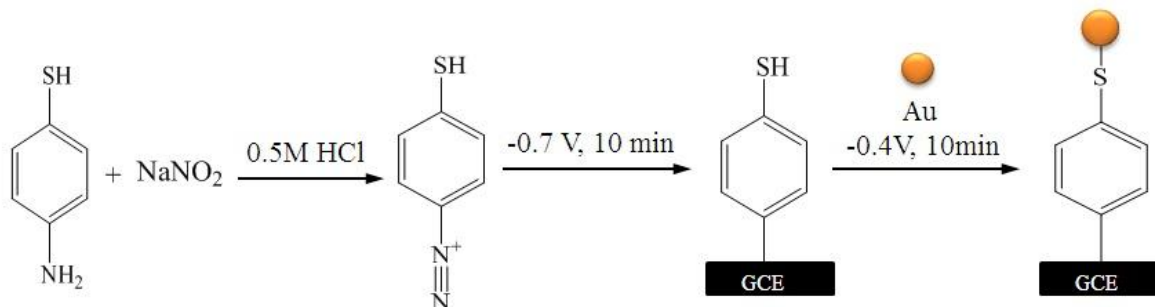
2.4 Characterization

Contact angle measurements were performed using a Phoenix 300 (Surface Electro Optics Co. Ltd.). The surfaces of the electrodes were investigated by an Atomic Force Microscopy, NanoScope V (Multi Mode), contact angle. X-ray photoelectron spectra of the samples were obtained using MultiLab ESCA2000 (Thermo Fisher Scientific, USA). Cyclic voltammetry was performed using a potentiostat Versa STAT3 (Princeton Applied Research). Electrochemical experiments were performed with a conventional three-electrode system. The glassy carbon electrode was used as the working electrode (diameter 2.0 mm). Platinum wire was used as a counter electrode. Electrochemical potentials were reported versus non-aqueous Ag/Ag⁺ and aqueous Ag/AgCl (sat'd KCl) reference electrodes. K₃[Fe(CN)₆] (1.0 mM) and K₄[Fe(CN)₆] (1.0 mM) (1:1) containing 0.1 M KCl was used as the supporting electrolyte.

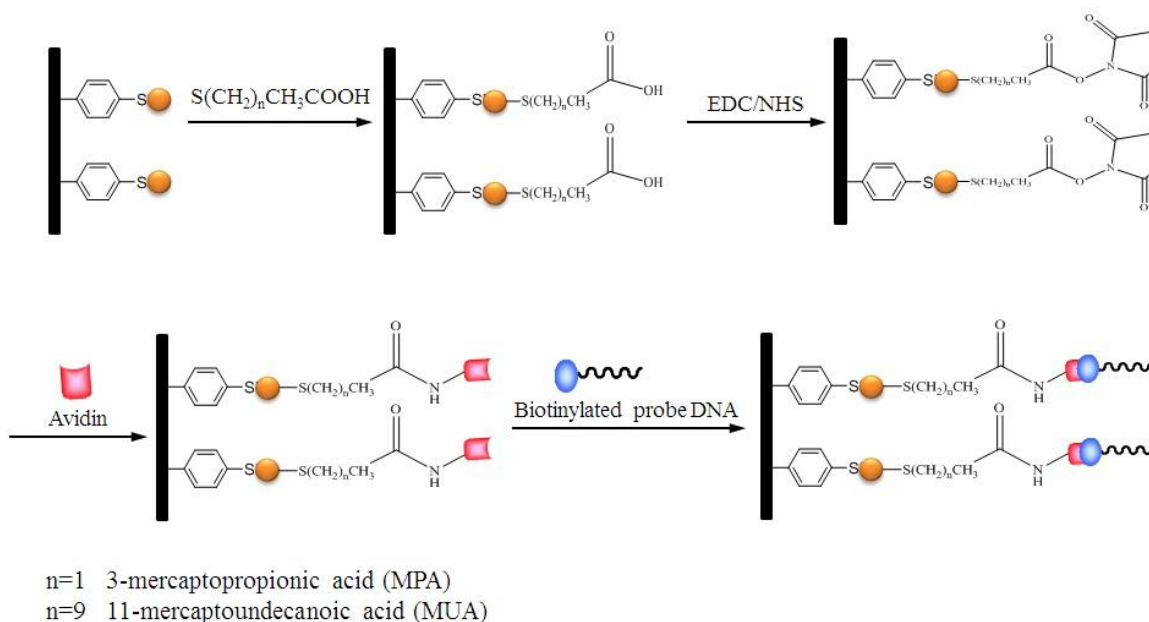
3. RESULTS AND DISCUSSION

First, an electrode was modified by electrochemical reduction of 4-aminothiophenol for 10 min in 0.5 M hydrochloric acid containing NaNO₂ at -0.7 V vs Ag/Ag⁺ as a reference electrode in order to

immobilize the thiol group onto surface of electrodes surface. For combination with Au NPs, subsequently the thiol-modified electrodes (TP-GCE) was immersed in H_2SO_4 solution containing hydrogen tetrachloroaurate(III) hydrate at 0.4 V for 10 min (Scheme 1). Then an E-DNA biosensor was fabricated using avidin-biotinlyted probe DNA conjugation (Scheme 2). The self-assembled monolayer (SAM) was formed on the Au NPs-modified electrode using one of the two molecules of MPA or MUA, which can induce avidin.



Scheme 1. Immobilization of Au on the surface of the GCE



► **Influenza virus (type A) DNA sequences.**

Biotinylated probe DNA : 5'-biotin-ATG AGT CTT CTA ACC GAG GTC GAA-3'

Target DNA : 5'-TTC GAC CTC GGT TAG AAG ACT CAT -3'

Two-base mismatch DNA : 5'-TTC GAC **AGC** GGT **TAT** AAG ACT CAT-3'

Scheme 2. Immobilization of probe DNA on the surface of the COOH-modified GCE in accordance with spacer

From SEM images (Fig. 1) to show changes in the surface of the electrode during the modification and immobilization steps, it can be seen that with the carbon plate as the model electrode (Fig. 1-a) the surface exhibits a smooth-like form and with the Au-TP-modified electrode (Fig. 1-b) the

appearance of the surface morphology shows crystal-like particles owing to immobilization of the Au NPs. After hybridization with DNA, there are no significant changes shown in either the MPA or MUA molecules with the probe DNA-MPA-Au-TP-modified electrode (Fig. 1-c) or probe DNA-MUA-Au-TP-modified electrode (Fig. 1-d) respectively.

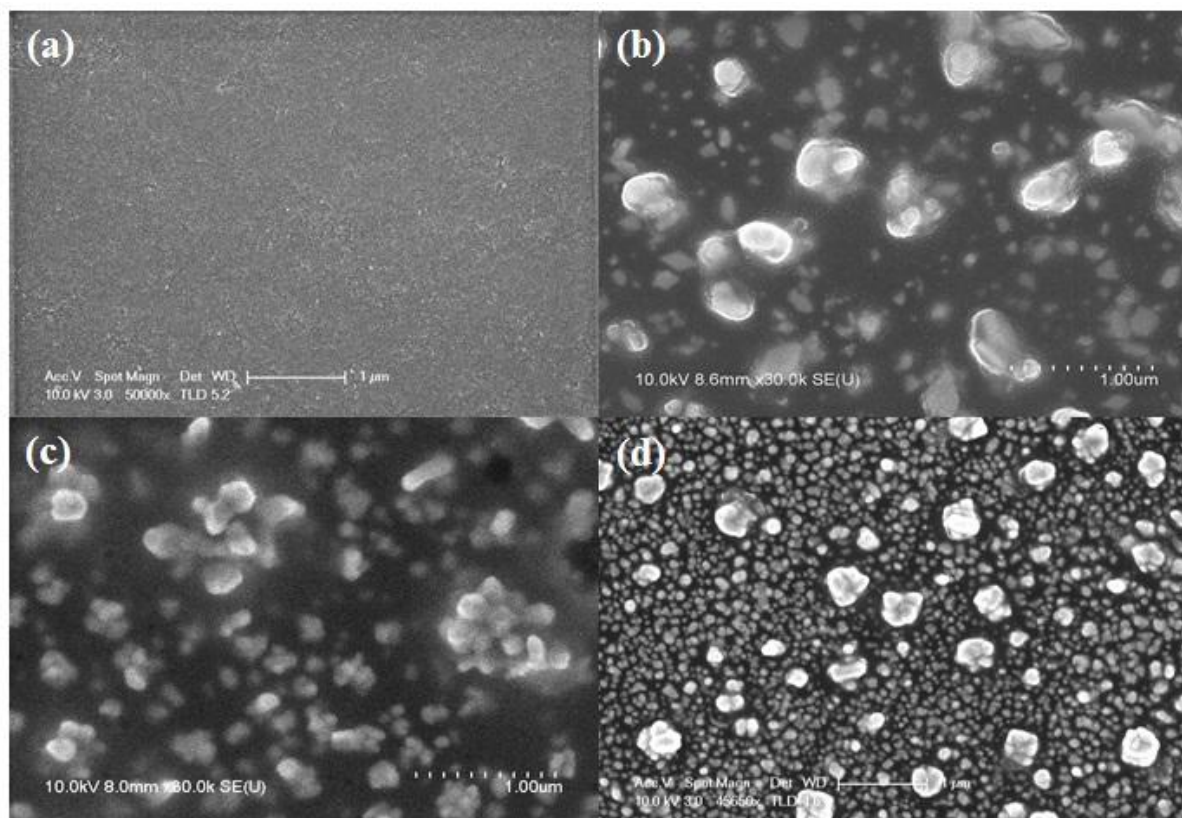


Figure 1. SEM images of the carbon plate as model electrode (a), Au-TP-modified electrode (b), probe DNA-MPA-Au-TP-modified electrode (c), and probe DNA-MUA-Au-TP-modified electrode (d).

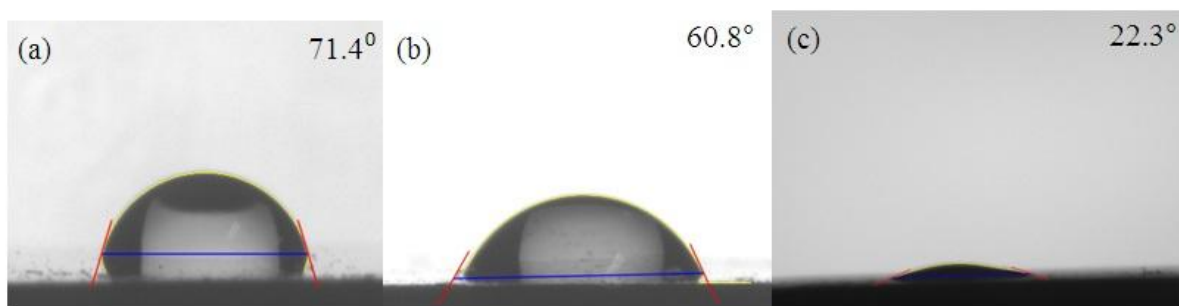


Figure 2. Contact angles of the carbon plate as model electrode (a), TP-modified electrode (b), and Au-TP-modified electrode (c).

From an examination of the water contact angles (Fig. 2), it is shown that the value of the contact angle of the carbon plate as model electrode was 71.4° (Fig. 2-a), while after electrochemical

reduction of 4-aminothiophenyl on the surface of the electrode the contact angle of the TP-modified electrode decreased to 60.8° (Fig. 2-b) and with the Au-TP-modified electrode the contact angle decreased further to 22.3° (Fig. 2-c) owing to immobilization of Au NPs onto the electrode. This result means that the carbon electrode was modified successfully by electrochemical reduction and immobilization of Au NPs; moreover, hydrophilicity was introduced to the surface. In order to confirm the introduction of the thiol group after electrochemical reduction, a surface analysis was performed. From the XPS survey scan spectra of the carbon plate as model electrode (Fig. 3-a), TP-modified electrode (Fig. 3-b), and Au-TP-modified electrode (Fig. 3-c), it can be seen that signals of S2p and Au4f appeared because of the modification and immobilization respectively using electrochemical reduction on the electrode. These results show that electrochemical modification with 4-thiophenyl diazonium salt on the surface of electrode was performed successfully, and that Au NPs were loaded by the thiol groups on the electrode. Moreover, high-resolution XPS spectra (Fig. 4) show that the peak of C1s was characterized by curve fitting. In the carbon plate as model electrode, the C1s peak could be decomposed into two contributions. The first signal at 284.9 eV is related to carbon involved in C-C and C-H bonds, while the other signal at 285.5 eV is attributed to C-O bonds. Meanwhile, the C1s peak in both the TP-modified electrode and Ag-TP-modified electrode could be decomposed into three contributions. The signals of C-N bonds and N1s appeared at 286.5 and 401.8 eV respectively owing to modification with 4-thiophenyl diazonium salts onto the electrode. The doublet XPS spectrum of S2p on the TP-modified electrode at 163.9 eV and 169.7 eV was confirmed, which is indicative for the signal of S in 4-thiophenyl groups, and unknown peak originated from disulfide or sulfide bond of conjugated aromatic polymer on the modified carbon electrode.

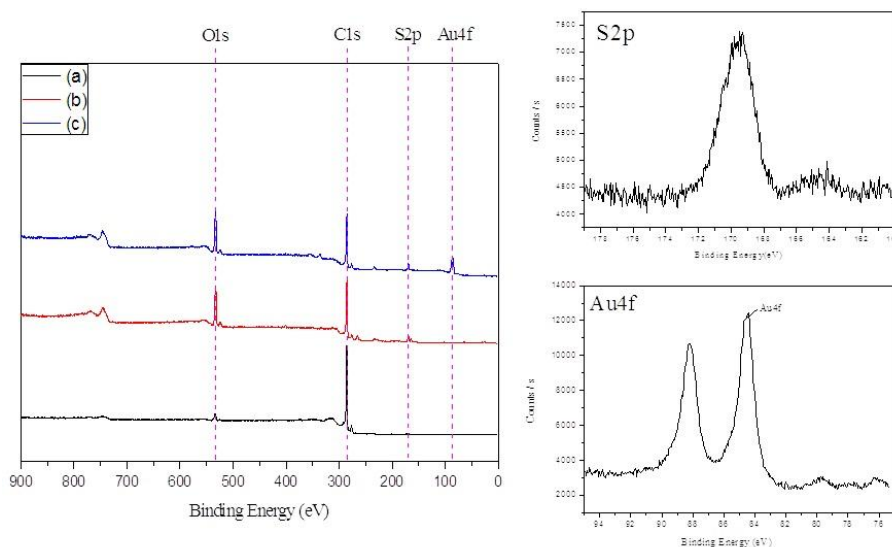


Figure 3. XPS survey scan spectra (left) of the carbon plate as model electrode (a), TP-modified electrode (b), and Au-TP-modified electrode (c). XPS scans on S2p and Au4f of the Au-modified electrode (right).

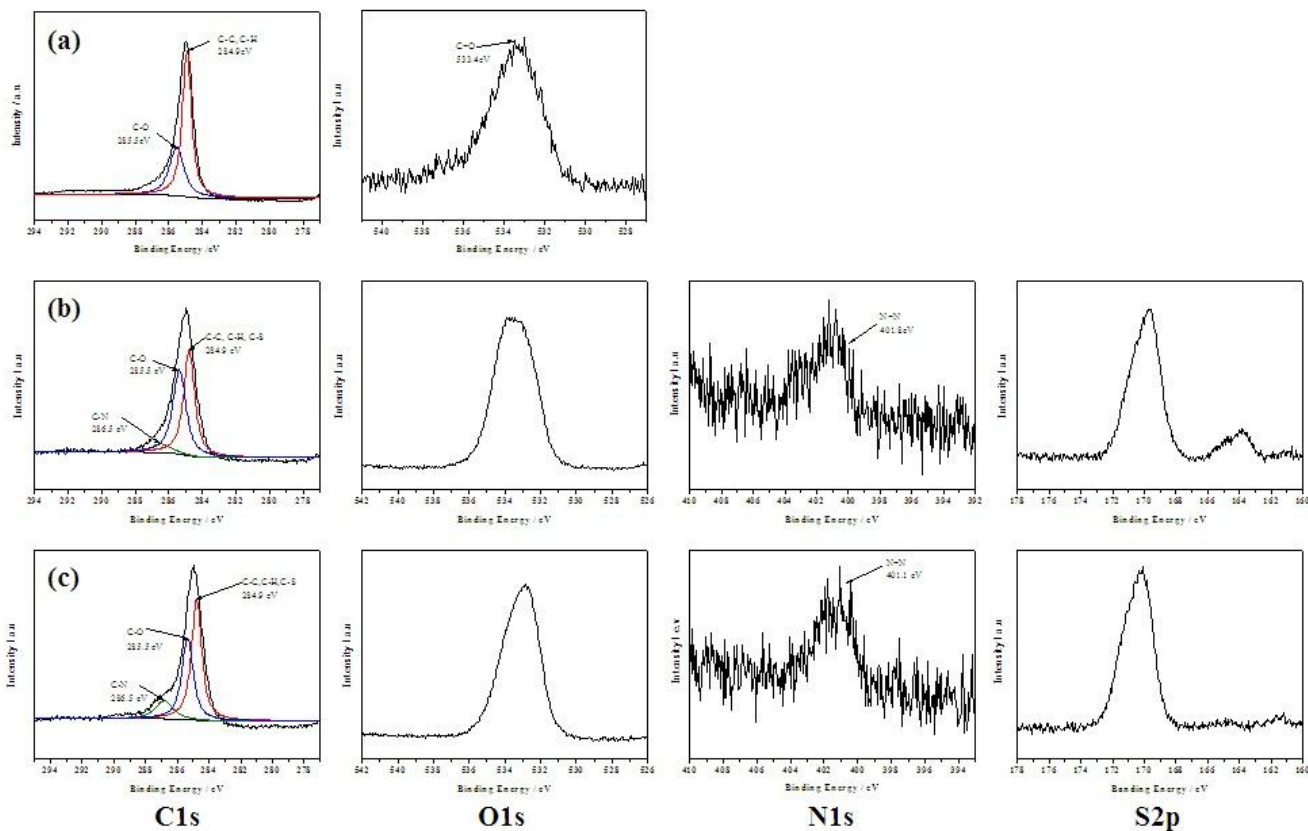


Figure 4. High-resolution XPS spectra of the carbon plate as model electrode (a), TP-modified electrode (b), and Au-TP-modified electrode (c).

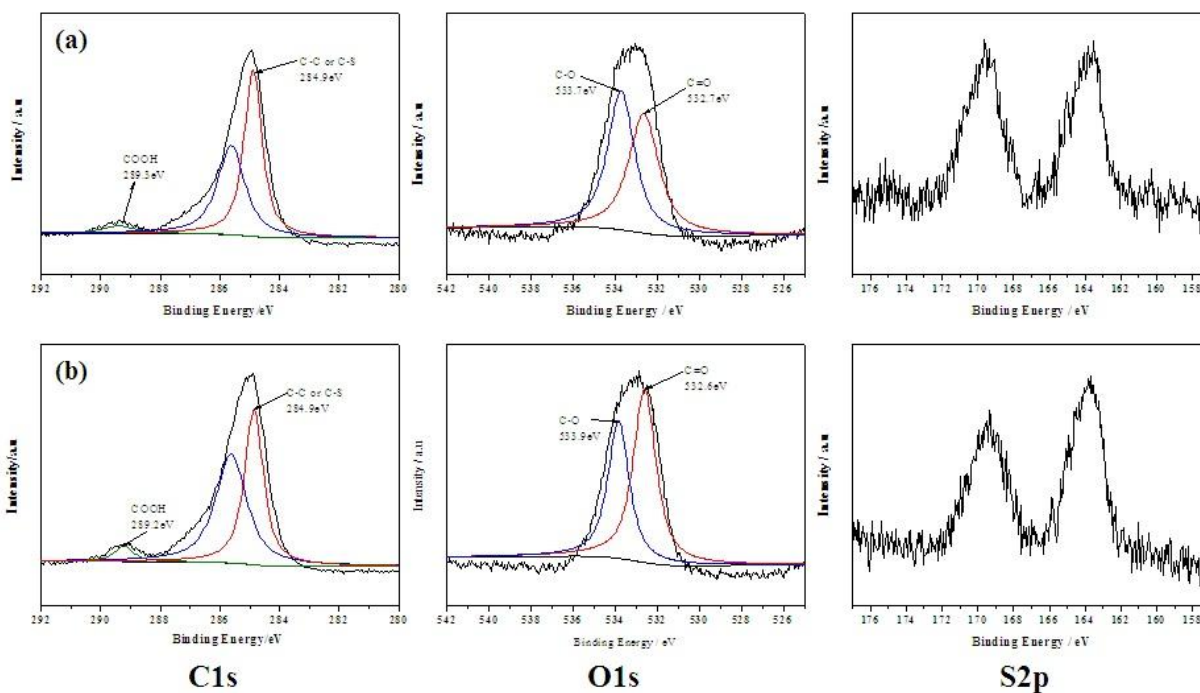


Figure 5. High-resolution XPS spectra of the MPA-Au-TP-modified carbon plate as model electrode (a) and MUA -Au-TP- modified electrode (b).

A self-assembled monolayer (SAM) was formed on Au-TP-modified electrode using two molecules of MPA and MUA in order to induce Avidin. Figure 5 shows the high-resolution XPS spectra of the MPS-Au-TP-modified carbon plate (Fig.5-a) and MUA-Au-TP-modified electrode (Fig. 5-b). In both the MPA-Au-TP-modified and MUA-Au-TP-modified electrode, the three peaks were appeared and assigned to, C-C, C-O, and -COOH features at 284.9, 289.2, and 289.1 eV, respectively. The appearance peak of -COOH was demonstrated that the SAM was successfully formed on Au-TP-modified electrode. In compared with Au-TP-modified electrode, the signal of S2p at 169.3 eV attributed to was increased due to the formation of SAMs on the electrode using MPA and MUA containing terminal thiol group.

intensity of peak at 163.9 eV attributed to unbounded sulfur was increased due to the formation of SAM on the electrode using MPA and MUA containing terminal thiol group. Moreover, the signal of bounded sulfur on Au NPs was not shown around 162 eV due to low intensity compared to the oxidized sulfur.

Figure 6 shows the AFM images of the carbon plate as model electrode (Fig. 6-a), TP-modified electrode (Fig. 6-b), and Au-TP-modified electrode (Fig. 6-c). It is well known that higher values for surface roughness can be explained by the inclusion of surface modifying materials. The value of surface roughness was 132.80 nm at the electrode before modification, increased to 169.25 nm because of modification using the electrochemical reduction of 4-thiophenyl diazonium, and increased further to 221.11 nm because of loading of Au NPs on the electrode. Also AFM images after immobilization of probe DNA on the electrode are shown in Figure 7. The values of surface roughness at the MPA-Au-TP-modified electrode and probe DNA-MPA-Au-TP-modified electrode were 311.11 and 701.38 nm respectively (Fig. 7 a-b), while those at the MUA-Au-TP-modified electrode and probe DNA-MUA-Au-TP-modified electrode were 590.17 and 893.92 nm respectively (Fig. 7 c-d), which shows clearly that higher surface roughness was achieved by the modification with MUA compared with MPA.

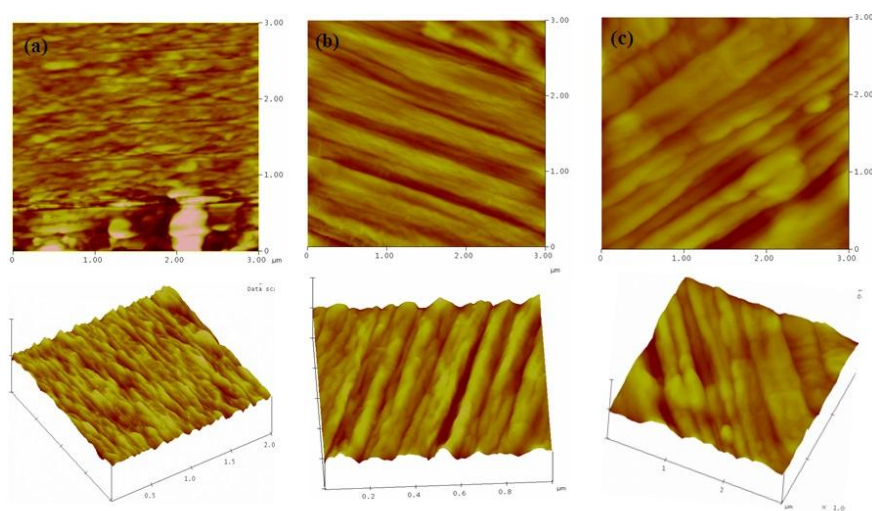


Figure 6. AFM images of the carbon plate as model electrode (a), TP-modified electrode (b), and Au-TP-modified electrode (c).

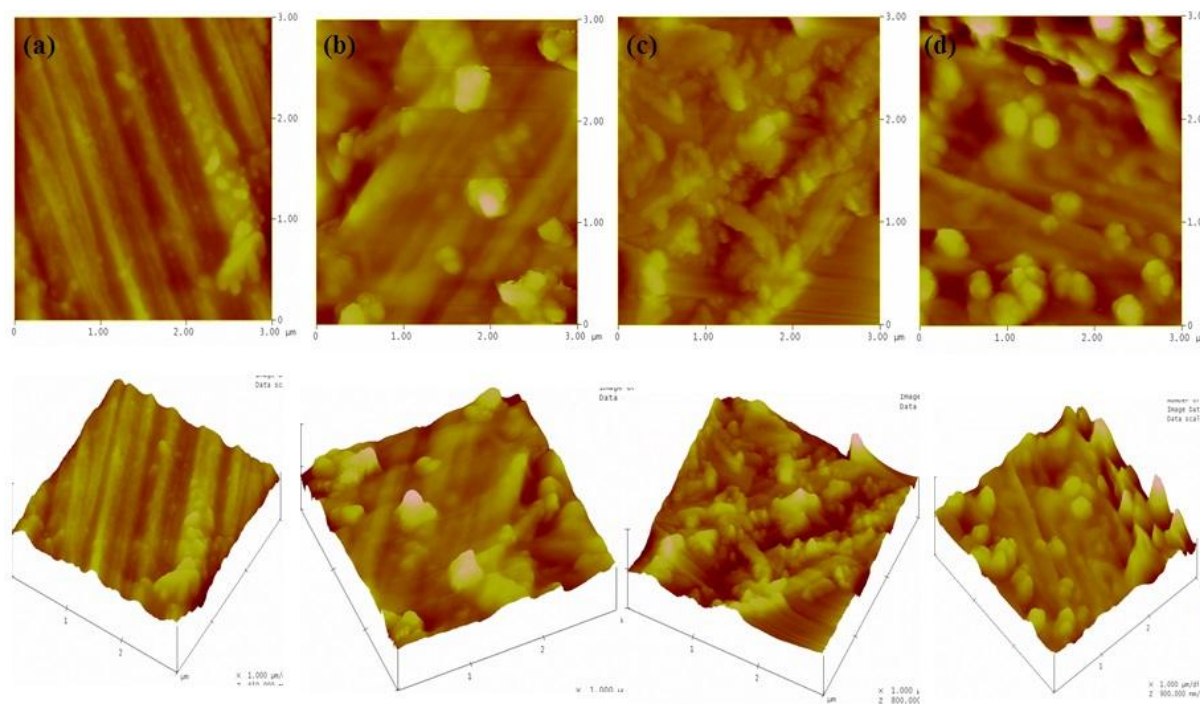


Figure 7. AFM images of the MPA-Au-TP-modified carbon plate as model electrode (a), probe DNA-MPA-Au-TP-modified electrode (b), MUA-Au-TP-modified electrode (c), and probe DNA-MUA-Au-TP-modified electrode (d).

In order to confirm the successful preparation in each step, the redox reaction was confirmed using cyclic voltammograms for each preparation step (Fig. 8). The cyclic voltammograms were recorded in 0.1 M KCl solution containing 1.0 mM $K_4Fe(CN)_6/K_3Fe(CN)_6$ (1:1) with a scan rate of 50 mV/s. In the bare GCE as a standard electrode, the peak-to-peak separation (ΔE_p) and the oxidation peak current were at 240 mV and 22.61 mA respectively. In comparison with the bare GCE, after modification with 4-thiophenyl diazonium (Fig. 8-b), the oxidation peak current was reduced by the formation of a small Faradic insulating-current layer of the 4-thiophenyl group on the electrode. Also, there was enhancement of the peak separation, ΔE_p , and the oxidation peak current at 270 mV and 26.04 mA respectively because the conductivity capability was enhanced by immobilization of the Au NPs (Fig. 8-c). After modification with MPA on the Au-TP electrode, the peak separation (ΔE_p) was increased to 470 mV and the oxidation peak current was reduced to 13.53 mA in comparison with the Au-TP electrode (Fig. 8-d) which indicates that electron transfer was interrupted by the SAM consisting of MPA layers. After the EDC and NHS treatment on the MPA-Au-TP electrode (Fig. 8-e), the oxidation peak current increased slightly because charge transfer occurred owing to tunneling of cationic NH^+ through the activated surface. After immobilization of the biotinylated DNA on the avidin-MPA-modified electrode (Fig. 8-g), the redox peak current changed remarkably because of an increase of electron transfer through the DNA chain. It is assumed that there was immobilization of probe DNA with modified electrode. As a result, an E-DNA biosensor based on an avidin-Au-modified electrode for influenza A virus (H1N1) detection was prepared successfully.

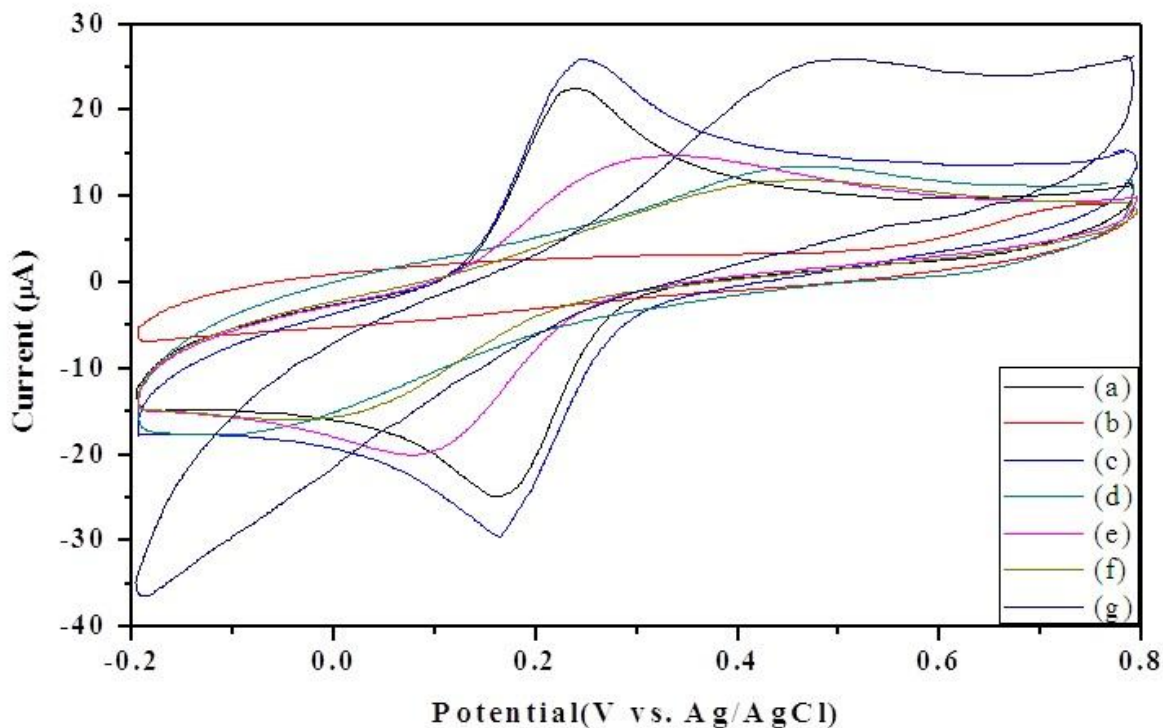


Figure 8. Cyclic voltammograms of bare GCE (a), TP-GCE (b), Au-TP-GCE (c), MPA-Au-TP-GCE (d), NHS/EDC-MPA-Au-TP-GCE (e), Avidin-NHS/EDC-MPA-Au-TP-GCE (f), and probe DNA-Avidin-NHS/EDC-MPA-Au-TP-GCE (g) in 0.1 M KCl solution containing 1.0 mM $K_4Fe(CN)_6 / K_3Fe(CN)_6$ (1:1) at a scan rate of 50 mV/s.

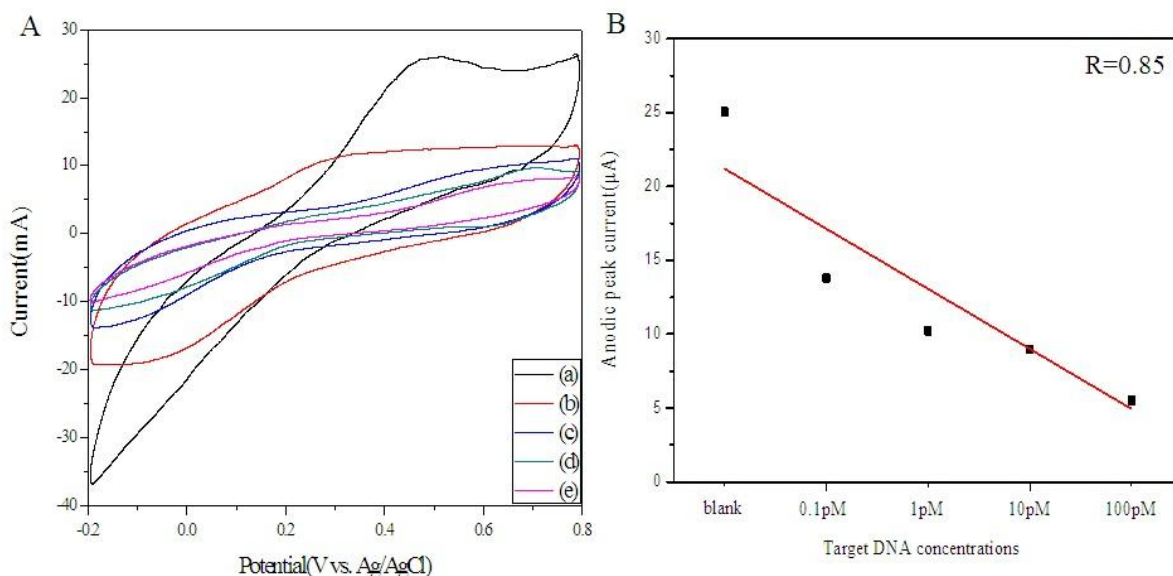


Figure 9. (A) Cyclic voltammograms of probe DNA-Avidin-NHS/EDC-MPA-Au-TP-GCE (a), and after hybridization reaction with the target DNA with different concentrations of 1.0×10^{-13} M (b), 1.0×10^{-12} M (c), 1.0×10^{-11} M (d), and 1.0×10^{-10} M (e) in 0.1 M KCl solution containing 1.0 mM $K_4Fe(CN)_6 / K_3Fe(CN)_6$ (1:1) at a scan rate of 50 mV/s. (B) Calibration curve of the current values with different concentrations of the target DNA.

The change in the surface current value of the E-DNA biosensor was expected and this was attributed to hybridization between the probe DNA and matching DNA in the electrolyte. After the hybridization reaction with the target DNA, the surface current value was determined by cyclic voltammograms as a function of various target DNA concentrations of 1.0×10^{-13} , 1.0×10^{-12} , 1.0×10^{-11} , and 1.0×10^{-10} M. The redox peak current was further reduced to a smaller value with increased concentration of target DNA as the probe DNA of the E-DNA biosensor was hybridized with the complementary target DNA with complementary target DNA (Fig. 9-A). A calibration curve of the current values with different concentrations of the target DNA (Fig. 9-B) shows that the oxidation current value between values from before and after hybridization was slightly linear with the logarithm of the target DNA concentration, and the regression coefficient was calculated as 0.85.

The cyclic voltammograms were prepared of the probe DNA-GCE (Fig. 10-a) and the electrode hybridized with two-base mismatched DNA (Fig. 10-b) and target DNA (Fig. 10-c) in 0.1 M KCl solution containing 1.0 mM $K_4Fe(CN)_6/K_3Fe(CN)_6(1:1)$ with a scan rate of 50 mV/s. When the probe DNA of the E-DNA biosensor was hybridized with complementary target DNA, the redox peak current was further reduced to a smaller value (Fig. 10-c). After the probe DNA of the E-DNA biosensor was hybridized with the two-base mismatched DNA sequence (Fig. 10-b), the redox peak current decreased owing to the presence of partial hybridization. In addition, there was a change in the redox peak current in the hybridization with the two-base mismatched DNA. These results demonstrate that the DNA-biosensor based on an avidin-MPA-modified electrode shows high selectivity for DNA hybridization detection.

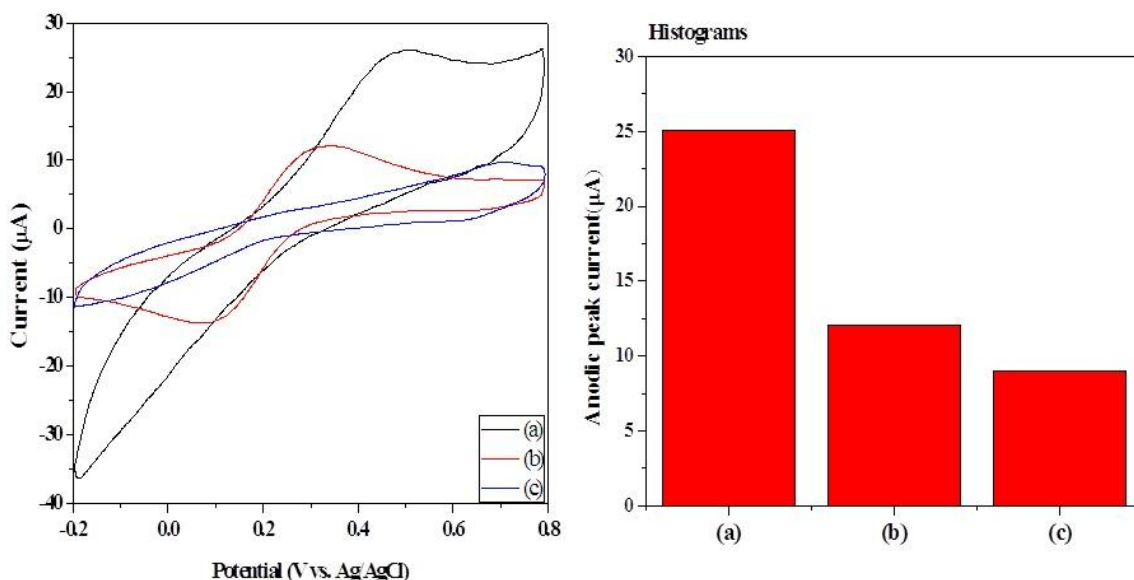


Figure 10. Cyclic voltammograms and histograms of probe DNA-Avidin-NHS/EDC-MPA-Au-TP-GCE (a) and the electrode hybridized with two-base mismatched DNA (1.0×10^{-11} M) (b) and target DNA (1.0×10^{-11} M) (c) in 0.1 M KCl solution containing 1.0 mM $K_4Fe(CN)_6/ K_3Fe(CN)_6$ (1:1) at a scan rate of 50 mV/s.

The redox reaction was also confirmed using cyclic voltammograms in order to demonstrate the effect of using MUA molecules for fabrication of an E-DNA biosensor. Cyclic voltammograms of the

electrode at each preparation step (Fig. 11) were recorded in 0.1 M KCl solution containing 1.0 mM $K_4Fe(CN)_6/K_3Fe(CN)_6$ (1:1) with a scan rate of 50 mV/s. The peak-to-peak separation (ΔE_p) and the oxidation peak current were 270 mV and 20.46 μA respectively. In comparison with the bare GCE, after modification with 4-thiophenyl diazonium (Fig. 11-b) the oxidation peak current was reduced by the formation of a small Faradic insulating-current layer of the 4-thiophenyl group on the electrode. Also, there was enhancement of the peak separation, ΔE_p , and the oxidation peak current enhanced at 280 mV and 24.47 μA respectively because of the loaded Au NPs on the electrode (Fig. 11-c). After modification with MUA on the Au-TP electrode, the redox peak current was reduced to a smaller value (Fig. 11-d) as the electron transfer was interrupted by the SAM consisting of MUA layers. After EDC and NHS treatment on the MPA-Au-TP electrode (Fig. 8-e), the oxidation peak current increased slightly because charge transfer occurred owing to tunneling of cationic NH^+ through the activated surface. After immobilization of biotinylated DNA on the avidin-MUA-modified electrode (Fig. 11-g), the redox peak current changed remarkably because of an increase of electron transfer through the DNA chain. It is assumed that there was immobilization of the probe probe DNA with the modified electrode. As a result, an E-DNA biosensor based on an avidin-Au-modified electrode for influenza A virus (H1N1) detection was prepared successfully.

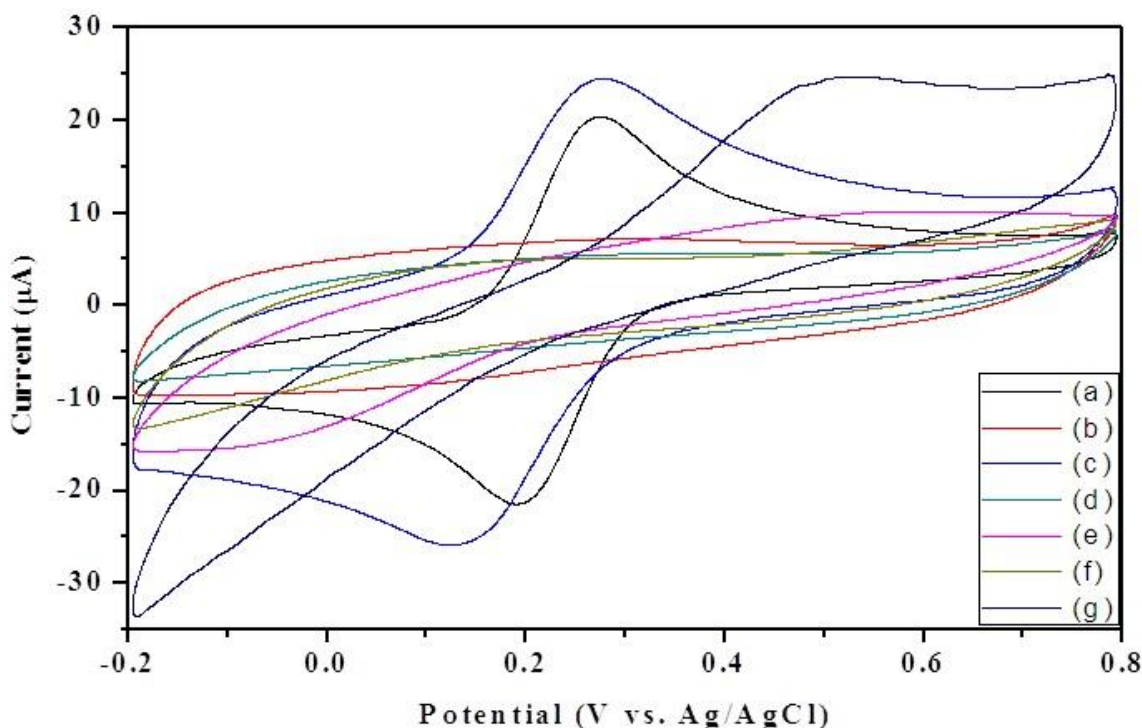


Figure 11. Cyclic voltammograms of bare GCE (a), TP-GCE (b), Au-TP-GCE (c), MUA-Au-TP-GCE (d), NHS/EDC-MUA-Au-TP-GCE (e), Avidin-NHS/EDC-MUA-Au-TP-GCE (f), and probe DNA-Avidin-NHS/EDC-MUA-Au-TP-GCE (g) in 0.1 M KCl solution containing 1.0 mM $K_4Fe(CN)_6/K_3Fe(CN)_6$ (1:1) at a scan rate of 50 mV/s.

The change in the surface current value of the E-DNA biosensor was expected and this was attributed to hybridization between the probe DNA and matching DNA in the electrolyte. First, cyclic

voltammograms were used to determine the surface current value as a function of various target DNA concentrations of 1.0×10^{-13} , 1.0×10^{-12} , 1.0×10^{-11} , and 1.0×10^{-10} M after the hybridization reaction with the target DNA. As can be seen from Figure 12-A, the results show that redox peak current was further reduced to a smaller value with increased concentration of the target DNA when the E-DNA biosensor was hybridized with the complementary target (Fig. 12-A). A calibration curve of the current values with different concentrations of the target DNA (fig. 12-B) shows that the oxidation current value between values from before and after hybridization was slightly linear with the logarithm of the target DNA concentration, and the regression coefficient was calculated as 0.97.

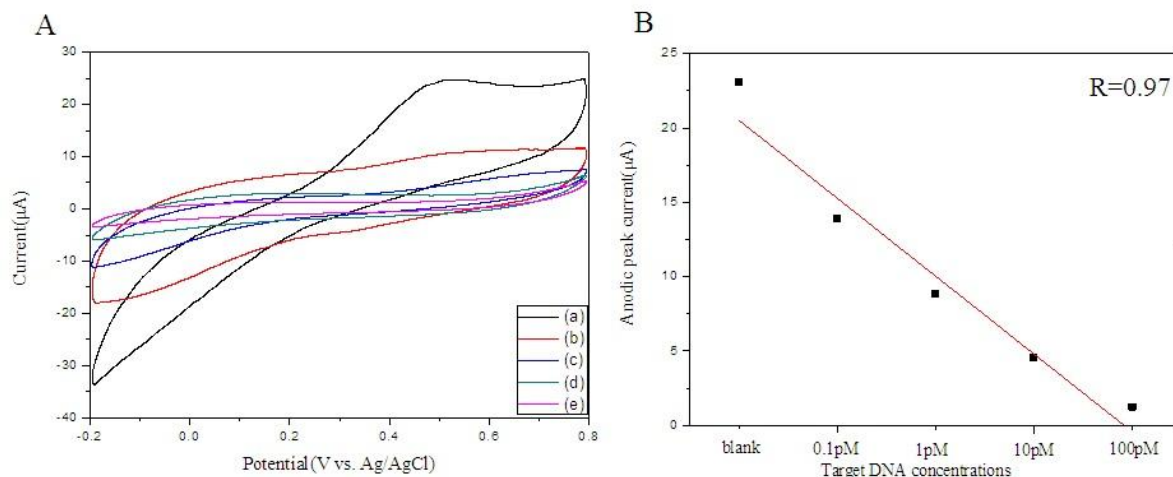


Figure 12. (A) Cyclic voltammograms of probe DNA-Avidin-NHS/EDC-MUA-Au-TP-GCE (a) and after hybridization reaction with the target DNA with different concentrations of 1.0×10^{-13} M (b), 1.0×10^{-12} M (c), 1.0×10^{-11} M (d), and 1.0×10^{-10} M (e) in 0.1 M KCl solution containing 1.0 mM $K_4Fe(CN)_6 / K_3Fe(CN)_6$ (1:1) at a scan rate of 50 mV/s. (B) Calibration curve of the current values with different concentrations of the target DNA.

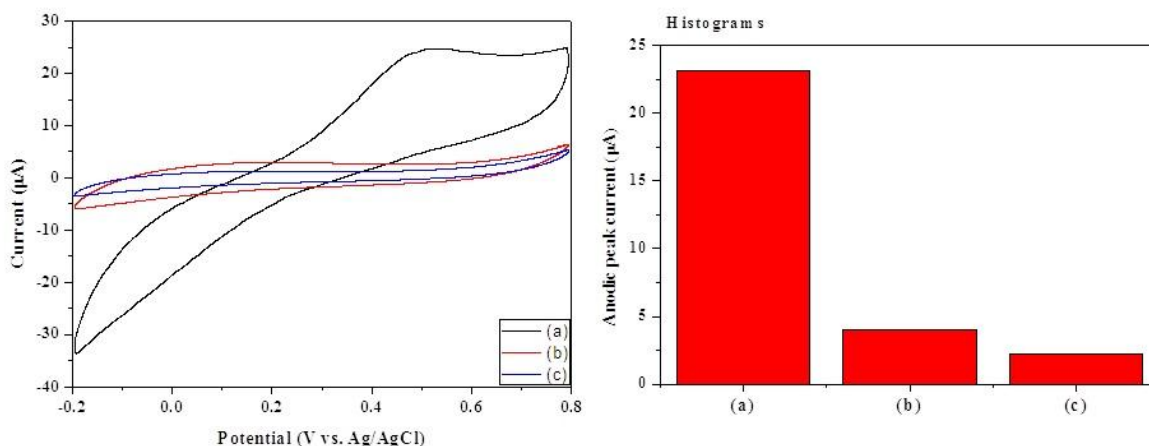


Figure 13. Cyclic voltammograms and histograms of probe DNA-Avidin-NHS/EDC-MUA-Au-TP-GCE (a) and the electrode hybridized with two-base mismatched DNA (1.0×10^{-11} M) (b) and target DNA (1.0×10^{-11} M) (c) in 0.1 M KCl solution containing 1.0 mM $K_4Fe(CN)_6 / K_3Fe(CN)_6$ (1:1) at a scan rate of 50 mV/s.

Figure 13 shows the cyclic voltammograms of the probe DNA-GCE (Fig. 13-a) and the electrode hybridized with two-base mismatched DNA (Fig. 13-b) and target DNA (Fig. 13-c) in 0.1 M KCl solution containing 1.0 mM $K_4Fe(CN)_6/K_3Fe(CN)_6$ (1:1) with a scan rate of 50 mV/s. After the probe DNA of the E-DNA biosensor was hybridized with the two-base mismatched DNA sequence (Fig. 13-b), the redox peak current decreased owing to the presence of partial hybridization. When the probe DNA of the E-DNA biosensor was hybridized with the complementary target DNA, the redox peak current was further reduced to a smaller value (Fig. 13-c). In comparison with the MPA-modified E-DNA biosensor (Fig. 10-c), the anodic peak current was further reduced to 2.27 μA for the MUA-modified E-DNA biosensor. These results demonstrate that the DAN-biosensor based on an avidin-MUA-modified electrode shows high sensitivity for DNA hybridization detection.

4. CONCLUSION

We prepared successfully an electrode that had its surface modified by a thiol group using 4-thiophenyl diazonium in a simple electrochemical reaction without any reducing agents. The characteristics of the modified electrode were obtained using cyclic voltammetry, contact angle, AFM, and XPS. As a result of this comprehensive treatment of the data, it was expected that the thiol-modified electrode would be a suitable material for performing further chemistry with residual grafted groups and other immobilized molecules. An E-DNA biosensor was prepared by electrochemical reduction and an avidin-biotinylated probe DNA conjugation. For the purpose of high electrical conductivity of the electrode, Au NPs were loaded on the thiol-modified electrode surface. Then SAM were formed on the electrode surface by one of the two molecules MPA or MUA in order to confirm the effective influence of the SAM layers on selectivity of the E-DNA biosensor. From the results, it was confirmed that the E-DNA biosensor based on an MUA-modified electrode showed higher sensitivity for hybridization between the probe DNA on the electrode and the target DNA compared with that based on the MPA-modified electrode because of the spacer effect occurring from the long chemical chain of the MUA molecules. The new E-DNA biosensor is considered to be one of the most promising materials for highly sensitive clinical and other biotechnology applications.

ACKNOWLEDGEMENT

This work was supported by the National Research Foundation of Korea Grant funded by the Korean Government (NRF-2013M1A3A3A02041878).

References

1. P.D. Tam, N.V. Hieu, N.D. Chien, A-T. Le M. A. Tuan, *J. Immunol. Methods* 350 (2009) 118.
2. F. Vianello, A. Cambria, S. Raqusa, M. T. Cambria, L. Zennaro, A. Rigo, *Biosens. Bioelectron.* 20 (2004) 315.
3. Y. Wan, Y. Su, X. Zhu, C. Fan, *Biosens. Bioelectron.* 47 (2013) 1.

4. D-J. Jung, S-H. Oh, S. Komathi, A. Gopalan, K-P. Lee, S-H. Choi, *Electrochim. Acta* 76 (2012) 394.
5. A.D. Chowdhury, R. Gangopadhyay, A. De, *Sensor. Actuat. B-Chem.* 190 (2014) 348.
6. N. Xia, D. Deng, L. Zhang, B. Yuan, M. Jing, J. Du, L. Liu, *Biosens. Bioelectron.* 43 (2013) 155.
7. D-J. Chung, K-C. Kim, S-H. Choi, *Appl. Surf. Sci.* 257 (2011) 9390.
8. A. K-Minkstimiene, A. Ramanaviciene, A. Ramanavicius, *Analyst* 134 (2009) 2051.
9. Y-F. Chang, S.F. Wang, J.C. Huang, L.C. Su, L. Yao, Y.C. Li, S.C. Wu, Y.M. Chen, J.P. Hsieh, C. Chou, *Biosens. Bioelectron.* 26 (2010) 1068.
10. J-E. Im, J-A. Ham, B.K. Kim, J-H. Han, T.S. Park, S. Hwan, S.I. Cho, W-Y. Lee, Y-R. Kim, *Surf. Coat. Tech.* 205 (2010) S275.
11. F. Li, Y. Feng, P. Dong, L. Yang, B. Tnag, *Biosens. Bioelectron.* 26 (2011) 1947.
12. B. Liu, L. Lu, M. Whang, Y. Zi, *J. Chem. Sci.* 120 (2008) 493.
13. G. Liu, J. Liu, T.P. Davis, J.J. Gooding, *Biosens. Bioelectron.* 26 (2011) 3660.
14. G. Liu, E. Luais, J.J. Gooding, *Langmuir* 27 (2011) 4176.
15. Y. Song, Z. Li, G. Wei, L. Wang, L. Sun, *Microsc. Res. Techniq.* 68 (2005) 59.
16. M. Kesik, F. E. Kanik, G. Hizalan, D. Kozanoglu, E.N. Esenturk, S. Timur, L. Toppare, *Polymer* 54 (2013) 4463.
17. R.K. Shervedani, S. Pourbeyram, *Sensors Actuators B* 160 (2011) 145.
18. T. Ahuja, V. K. Tanwar, S. K. Mishra, D. Kumar, A. M. Biradar, Rajesh, *J. Nanoscience. Nanotechnology.* 11 (2011) 4692.
19. A. Hayat, L. Barthelmebs, J-L Marty, *Sensors. Actuat. B-Chem.* 171-172 (2012) 810.
20. A. Hayat, L. Bathelmebs, A. Sassolas, J.L. Marty, *Talanta* 85 (2011) 513.
21. J. W. Park, H. S. Jung, H. Y. Lee, T. Kawai, *Biotechnol. Bioprocess. Eng.* 10 (2005) 505.
22. C.M. Whelan, M.R. Smyth, C.J. Barnes, N.M.D. Brown, C.A. Anderson, *Appl. Surf. Sci.* 134 (1998) 144.
23. A. Francesko, D.S. Costa, P. Lisboa, R.L. Reis, I. Pashkuleva, T. Tzanov, *J. Mater. Chem.* 22 (2012) 19438.
24. B. Genorio, T. He, A. Meden, S. Polanc, J. Jamnik, J.M. Tour, *Langmuir* 24 (2008) 11523.